

Visual Topography of Striate Projection Zone (MT) in Posterior Superior Temporal Sulcus of the Macaque

RICARDO GATTASS AND CHARLES G. GROSS

Department of Psychology, Princeton University, Princeton, New Jersey 08544

SUMMARY AND CONCLUSIONS

1. The representation of the visual field in the striate projection zone in the posterior portion of the superior temporal sulcus of the macaque (MT) was mapped with multiunit electrodes. The animals were immobilized and anesthetized and in each animal 25–35 electrode penetrations were typically made over several recording sessions.

2. MT contains a representation of virtually the entire contralateral visual field. The representation of the vertical meridian forms its ventrolateral border and lies near the bottom of the lower bank of the superior temporal sulcus (STS). The representation of the horizontal meridian runs across the floor of STS. The upper field is located ventral and anterior and the lower field dorsal and posterior. The medial border lies at the junction of the floor of STS and its upper bank.

3. MT is similar to striate cortex in being a first-order transformation of the visual field. In both areas, receptive-field size and cortical magnification increase with eccentricity. MT is much smaller than striate cortex and has much larger receptive fields at a given eccentricity and a cruder topography.

4. The results further support the suggestion that MT in the macaque is homologous to visual area MT in New World primates.

INTRODUCTION

Several studies (6, 17, 19, 20, 22–24, 32, 33, 35–39, 41) have demonstrated that striate cortex in the macaque projects to a limited area in the posterior portion of the superior temporal sulcus (STS). Zeki (43)

has termed this area the motion-sensitive area of STS because its neurons are particularly sensitive to the direction of stimulus movement. Allman (1), Weller and Kaas (36), and Van Essen, Maunsell, and Bixby (33) have called it MT because there are several lines of evidence that it is homologous to the middle temporal visual area (MT) of the owl monkey (1, 32). Although MT in the macaque is not in the middle of the temporal lobe, we will use this designation to avoid further multiplication of names, because of its brevity, and because there are other motion-sensitive areas in STS (5).

Zeki (39) originally described the organization of MT as nontopographic. However, recent anatomical and physiological evidence from his and other laboratories has indicated that it has at least some retinotopic organization (22–24, 32, 35, 40, 43). This organization has been variously described as crude (40), complex (22), and containing multiple rerepresentations of the visual field (43).

On the basis of recordings from small groups of neurons, we report on the visual organization of MT. It contains a single representation of the contralateral visual field. The overall organization of MT is similar to that of striate cortex but the representation of the visual field is much coarser.

A preliminary report of these results has appeared elsewhere (11).

METHODS

Animal preparation and maintenance

Six *Macaca fascicularis* weighing between 3.0 and 4.8 kg were used. Five were recorded from on eight occasions and one twice. All recordings from an individual animal were made within a 4-

wk period. Prior to the first recording session, a stainless steel recording well (3.5-cm diameter) and a bolt for holding the animal in a stereotaxic machine were implanted under aseptic conditions under pentobarbital anesthesia.

The treatment of the animals in each recording session has been described in detail previously (9). Briefly, in each session, after injections of atropine and diazepam, the animals were restrained with ketamine hydrochloride, anesthetized with a mixture of halothane, nitrous oxide, and oxygen, intubated with a tracheal tube, fixed in the stereotaxic machine by the head bolt, immobilized with pancuronium bromide, and maintained under 70% nitrous oxide and 30% oxygen. End-tidal CO_2 , body temperature, and heart rate were continually monitored. The pupils were dilated with cyclopentolate hydrochloride and the corneas covered with contact lenses. After about 13 h, infusion of the paralyzing agent was terminated and the animal returned to its cage about 4 h later. At least 2 days separated successive recording sessions.

Recording

Varnish-coated tungsten microelectrodes with exposed tips of 20–50 μm and 2- to 6-M Ω impedance were used. These electrodes recorded action potentials from several neurons or "multiunits." In a typical animal, 25–35 vertical electrode penetrations were made over the 4-wk recording period. They were spaced approximately 1–1.5 mm apart, forming a grid extending throughout MT and adjacent areas. On each penetration, recording sites were separated by a minimum of 400 μm .

Visual stimuli

The nodal point of the eye contralateral to the recording sites was placed at the center of a 120-cm-diameter translucent plastic hemisphere. The cornea was covered with a contact lens selected by retinoscopy to focus the eye at 60 cm. The locations of the fovea and the center of the optic disk were projected onto the hemisphere. The horizontal meridian was defined as a line passing through both these points and the vertical meridian as an orthogonal line passing through the fovea. The ipsilateral eye was occluded.

Since the eye was paralyzed, we did not stimulate portions of the retina obscured by the nose and orbital ridge. The maximum extent of the exposed visual field was estimated from the visual angles at which the reflections (Purkinje images) of a small light source disappeared from the eye while sighting along the visual axis. In our paralyzed preparation, the maximum extent of visual stimulation along the horizontal meridian was about 100° from the vertical meridian and along the vertical meridian about 55° in the upper visual field and 60° in the lower. Thus, reference to the

complete visual field or to either entire meridian includes only these exposed dimensions.

The usual stimuli used for receptive-field mapping consisted of white and colored bars (0.7–0.18 ft candle) rear projected onto the hemisphere under low ambient light (0.04 ft candle) or opaque objects moved along the hemisphere under high ambient light (0.2 ft candle). Typically, the projected stimuli subtended 3.7° x 0.7°.

Histology

Small electrolytic lesions were made at several recording sites on each penetration by passing a direct current (4 μA for 20 s) through the microelectrode. At the end of the final session the animal was anesthetized with sodium pentobarbital and perfused with saline followed by buffered Formalin. After removal the brain was photographed and cast in dental-impression compound. After sinking in sucrose Formalin, 33.3- μm frozen sections were cut. Four brains were cut in the coronal plane, one in the sagittal plane, and one at 20° to the vertical. Alternate sections were stained for cell bodies with cresyl violet and for fibers with a modified Heidenhain-Woelke stain.

The modified Heidenhain-Woelke, unlike the Weil and Spielmeyer stains, does not use either borax or ferric ammonium sulfate in the differentiation process. Unmounted sections fixed with 10% Formalin were rinsed in distilled water for 2 h and left overnight in the mordant solution (2.5% ferric ammonium sulfate) in the dark. After a quick rinse in distilled water, the sections were placed into fresh stain (300 ml H_2O , 60 ml filtered, aged hematoxylin 10% in ethanol, and 12.5 ml of saturated lithium carbonate) and placed on a rocker for 2 h. After rinsing 4 times with distilled water (30 s each), the sections were differentiated in 70 and 80% ethanol (10–15 min each). After "stabilizing" the stain with 95% ethanol, the sections were rehydrated (70 and 80% ethanol, 2 min each) and immediately mounted in ethanol (40%-gelatin (0.25%). The sections were then dehydrated in 95 and 100% ethanol (3 min each), cleared in xylene (2 x 3 min), and cover slipped. The differentiation is highly dependent on the amount of lithium carbonate in the stain and test sections are required. This staining procedure is unusually hard on the sections, and the quality of the staining varies from animal to animal.

RESULTS

Visual topography

In this portion of the RESULTS, we first summarize the location and overall topographic organization of MT. Second, we give examples of the relationship between recording sites and the location of the receptive

fields recorded at those sites. Then we show how such data were used to construct maps of the visual topography of MT. In subsequent portions of the RESULTS we consider receptive-field size and cortical magnification as a function of eccentricity, and then the architectonic correlates of MT.

LOCATION AND OVERALL ORGANIZATION. MT is an oval-shaped area of about 80 mm² in the lower bank and floor of the posterior portion of the superior temporal sulcus. In the animals studied it was always posterior to an imaginary line connecting the dorsal tip of the inferior occipital sulcus and the anterior tip of the intraparietal sulcus and never extended to the lip of either the lower or upper bank of the superior temporal sulcus (Figs. 1 and 5*B*).

MT contains a representation of virtually the entire visual field. The representation of the vertical meridian forms the ventrolateral border of MT and lies near the bottom of the lower bank of STS. The representation of the horizontal meridian runs obliquely and anteriorly across the floor of STS. The upper visual field is located ventroanteriorly and the lower visual field dorsoposteriorly. The representation of the central 5° is greatly magnified. This representation of the visual field is an example of what Allman and Kaas (2) have termed a first-order representation, that is, a simple topological representation in which adjacent points in the

contralateral half-field are represented in adjacent cortical loci.

RECEPTIVE-FIELD SEQUENCES IN CORONAL AND SAGITTAL SECTIONS. Figure 2 illustrates the location of receptive fields recorded in a series of penetrations in the coronal plane. If we start in the bottom of the lower bank of STS (Fig. 2*C*) and move medially across the floor to the bottom of the upper bank, the centers of receptive fields recorded at these sites show a systematic progression through the visual field (Fig. 2*D*). In the lower bank of STS, the receptive fields in MT are in the upper visual field near the fovea (sites 3–5). As we move medially across the floor, the receptive fields cross the horizontal meridian (sites 4–7) and move into the periphery of the lower visual field (sites 8–11).

Although the general progression of receptive-field centers as we move across the floor of the sulcus is from the vertical meridian into the periphery, the progression is occasionally irregular and reverses itself. Note that the receptive-field sizes grow very rapidly with increasing eccentricity and that the receptive fields with centers beyond 10° are so large that their medial borders sometimes approach or reach the vertical meridian (Fig. 2*F*).

In this section, MT is bordered by visually responsive cortex, which is myeloarchitectonically distinguishable from MT. Lateral to MT in the upper portion of the lower bank of STS, the receptive-field progression reverses and moves away from the vertical meridian (Fig. 2*E*, sites 2–1). Medial to MT in the upper bank of STS (sites 12–14), the fields are larger than in MT and extend well into both the upper and lower visual fields. This area falls within Brodman's area 7 and does not appear to be topographically organized.

An identical progression of receptive fields from the center of the visual field to the periphery as we move from lateral to medial sites in MT in another animal is shown in Fig. 12. This figure also demonstrates reversals in the progression of receptive-field centers at the lateral border of MT.

Figure 3 illustrates the location of receptive fields recorded in three penetrations in the parasagittal plane along the posterior

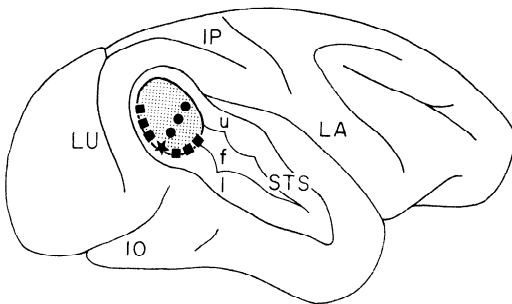


FIG. 1. Lateral view of the macaque brain with the superior temporal sulcus (STS) opened showing its upper bank (u), floor (f), and lower bank (l). The striate projection zone in the posterior superior temporal sulcus (MT) is shown in gray, the representation of the vertical meridian with squares, that of the horizontal meridian with circles, and that of the center of gaze with a star. IO, inferior occipital sulcus; IP, intraparietal sulcus; LA, lateral sulcus; LU, lunate sulcus.

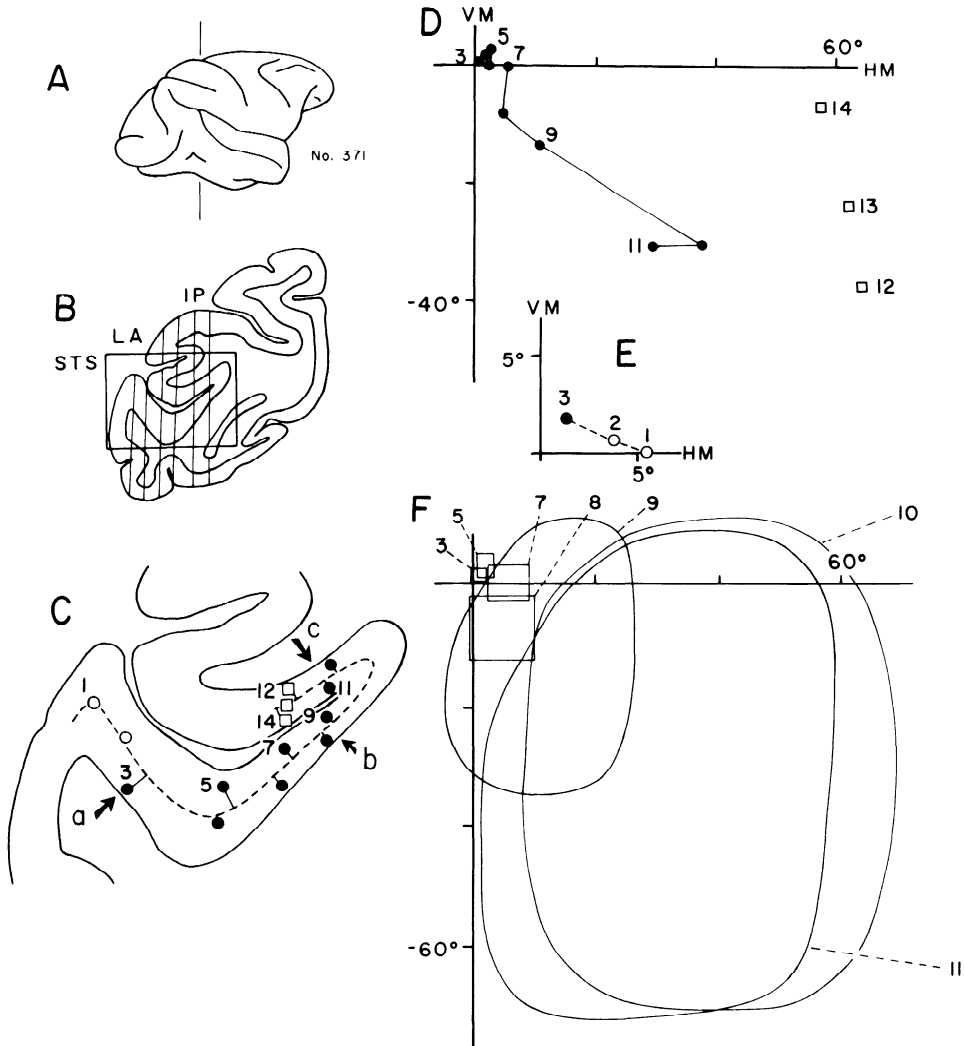


FIG. 2. Receptive fields in MT and adjacent areas recorded in a series of penetrations in the coronal plane. *A*: lateral view of the brain showing level of the section. *B*: coronal section showing electrode tracks and the portion enlarged in *C*. *C*: enlarged portion of STS indicating the recording sites outside (open circles and squares) and inside MT (filled circles) projected onto layer IV (dashed line). Limits of MT determined by myeloarchitectonic criteria are shown by arrows *a* and *c*. Arrow *b* indicates the transition from heavy (below) to lighter myelination. *D* and *E*: receptive-field centers recorded at sites shown in *C*. *F*: receptive fields recorded in MT at sites shown in *C*. A few receptive fields have been omitted for clarity. VM, vertical meridian; HM, horizontal meridian. See also legend to Fig. 1.

bank of STS. As we move from posterior to anterior sites within MT (from sites 5 to 14), the receptive fields move from the periphery of the lower visual field, across the horizontal meridian into the upper visual field, and then toward the vertical meridian. The progression toward the vertical meridian in the upper field (sites 10–14) reflects the expansion

of the representation of the central visual field and its ventral location. As in the coronal section, the more peripheral fields are larger (Fig. 3*E*) and the progression zigzags somewhat.

Crossing the posterior border of MT onto the prelunate gyrus, we move into V4 (sites 4–1) and the progression of receptive-field

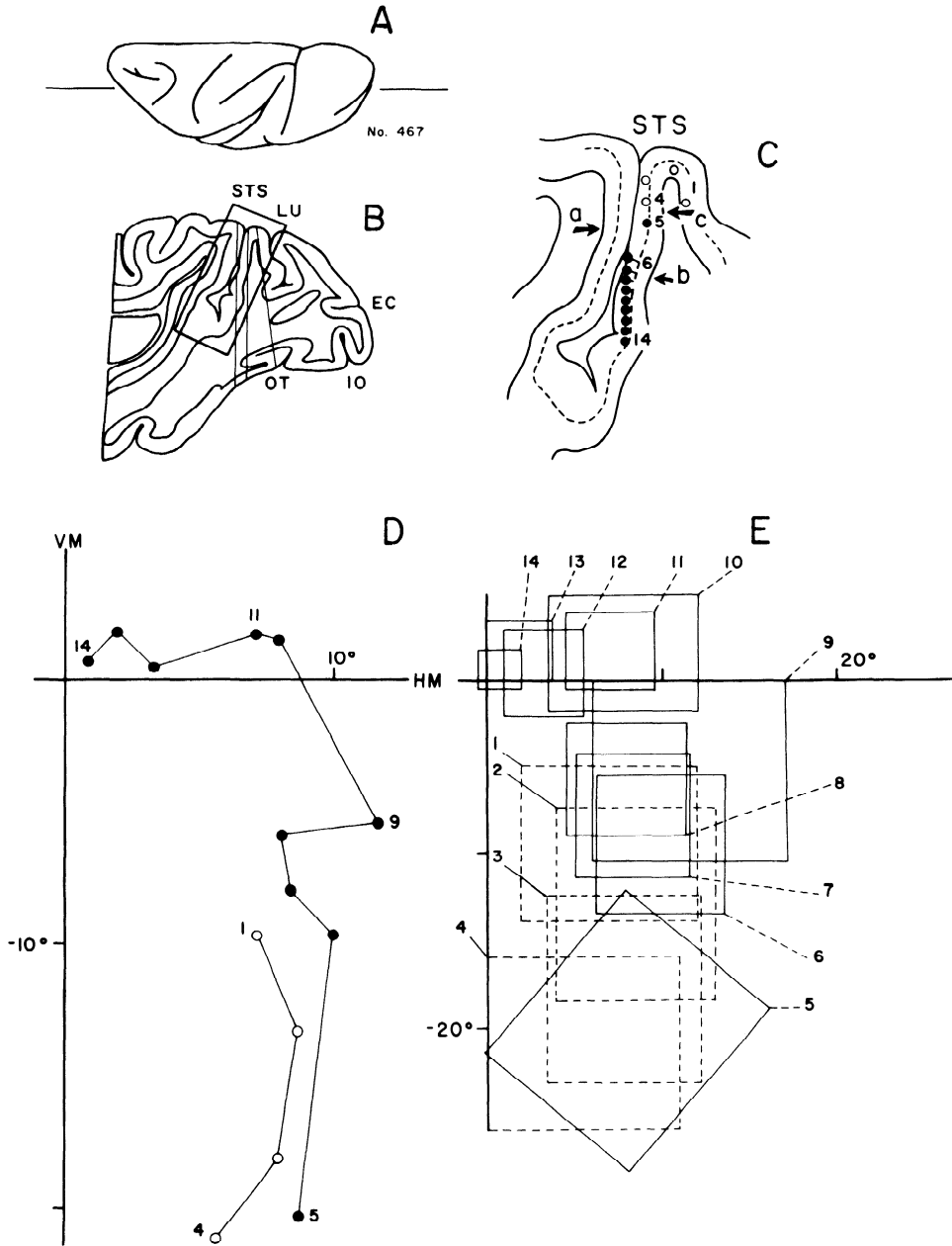


FIG. 3. Receptive fields in MT and adjacent area recorded in a series of penetrations in the parasagittal plane. *A*: dorsal view of the brain showing level of the section. *B*: sagittal section showing the electrode tracks and the portion enlarged in *C*. *C*: enlarged portion of STS showing recording sites outside (open circles) and inside (filled circles) MT projected onto layer IV. Arrows *a* and *c* show limits of MT myeloarchitectonically determined. Arrow *b* indicates the transition from heavy (below) to lighter myelination. *D*: receptive-field centers recorded at sites shown in *C*. *E*: receptive fields in MT (solid lines) and outside MT (dotted lines) at sites shown in *C*. EC, external calcarine sulcus; OT, occipitotemporal sulcus. See also legend to Fig. 1.

centers reverses, but receptive-field size remains similar (Fig. 3*E*).

In summary, at these levels as we move

lateromedially in MT, the receptive fields move from the central vertical meridian into the periphery (Figs. 2 and 12); as we move

posteroanteriorly, they move from the lower visual field into the upper visual field (Fig. 3).

VISUOTOPIC ORGANIZATION OF MT. In order to transform data such as those shown in Figs. 2 and 3 into a "map" of the visual topography of MT, we first unfolded the relevant portions of STS by building a three-dimensional model and then flattening it. Sections through STS were traced at 10 \times magnification and a wire bent to conform to layer IV of each section. The wires were then attached with scaled cross pieces to form a three-dimensional model of the banks and floor of STS. The model was then unfolded (flattened) by hand, cutting the minimum number of cross pieces to form a two-dimensional surface. Flattened models are illustrated in Figs. 4*B*, 5*A*, and 6.

Each recording site was projected orthogonal to the cortical surface onto layer IV and then marked on the flattened model. (The orthogonal projection was measured in the plane of section by visual inspection and the plane orthogonal to the plane of section by reconstruction from adjacent sections.) The vertical and horizontal coordinates of the receptive-field centers recorded at each site were marked on the map and on the basis of these coordinates the location of the vertical and horizontal meridians were drawn. Similarly, the eccentricity of the receptive-field centers recorded at each site were marked on the flattened model and isoeccentricity lines drawn.

Some of the stages in the production of a map of the visual topography of MT in one animal (437) are shown in Fig. 4. In Fig. 4*B*, the locations of the recording sites in MT are shown and numbered on a flattened model. The locations of the receptive-field centers recorded at each of these sites are shown in Fig. 4*C* (for the central 2 $^\circ$) and Fig. 4*D* (for the rest of the visual field). In Fig. 4*E*, the eccentricity, in degrees, of the receptive-field centers recorded at each site are indicated along with 2, 10, and 30 $^\circ$ isoeccentricity lines drawn by eye to fit the eccentricity values indicated. The derivation of the meridians was similar to that of the isoeccentricity lines but is not illustrated. In Fig. 5*A* the isoeccentricity lines are combined with the meridians to provide a map

of the overall visual topography of MT in this animal (Fig. 5*B* is a three-dimensional drawing of MT in this animal). Since the position of the isoeccentricity lines and meridians were estimated by eye, slightly different ones could be drawn that would fit the data about as well, but the overall topography summarized in Fig. 5 would be altered little by these variations. Maps derived in an identical fashion for three other animals are shown in Fig. 6.

In spite of the interanimal variation in sulcal morphology, the maps shown in Figs. 5 and 6 and those from the other two animals are basically similar. (The most deviant one is from animal 369, shown in Fig. 6. In this animal STS has an additional small branch or dimple in the region of MT and this complexity made the unfolded map somewhat distorted.) In each animal, the representation of the vertical meridian forms the ventrolateral border of MT and lies near the bottom of the lower bank of STS and the representation of the horizontal meridian crosses the floor of STS. The upper visual field is located ventral and anteriorly, and the lower visual field dorsal and posteriorly.

Figure 7 illustrates the total area of the visual field included in the receptive fields recorded in MT of animal 437. In this and the other animals, essentially the entire contralateral visual field and at least 5 $^\circ$ of the ipsilateral visual field are represented. However, receptive-field centers did not extend beyond an eccentricity of about 55 $^\circ$. Rather, the more peripheral portions of the visual field were included within the large receptive fields whose centers had eccentricities of 30–50 $^\circ$. Similarly, there were virtually no receptive fields whose centers were on or near the vertical meridian beyond an eccentricity of 5–10 $^\circ$. Rather, the more peripheral portions of the vertical meridian were included within large receptive fields whose centers lay 5 $^\circ$ or more from the vertical meridian. (In Figs. 5 and 6 we have marked as the representation of the vertical meridian only the sites at which the centers of the receptive fields were on or close to the vertical meridian.) In fact the entire vertical meridian was "represented" within MT.

The different portions of the visual field are not uniformly represented in MT. The representation of the central visual field is

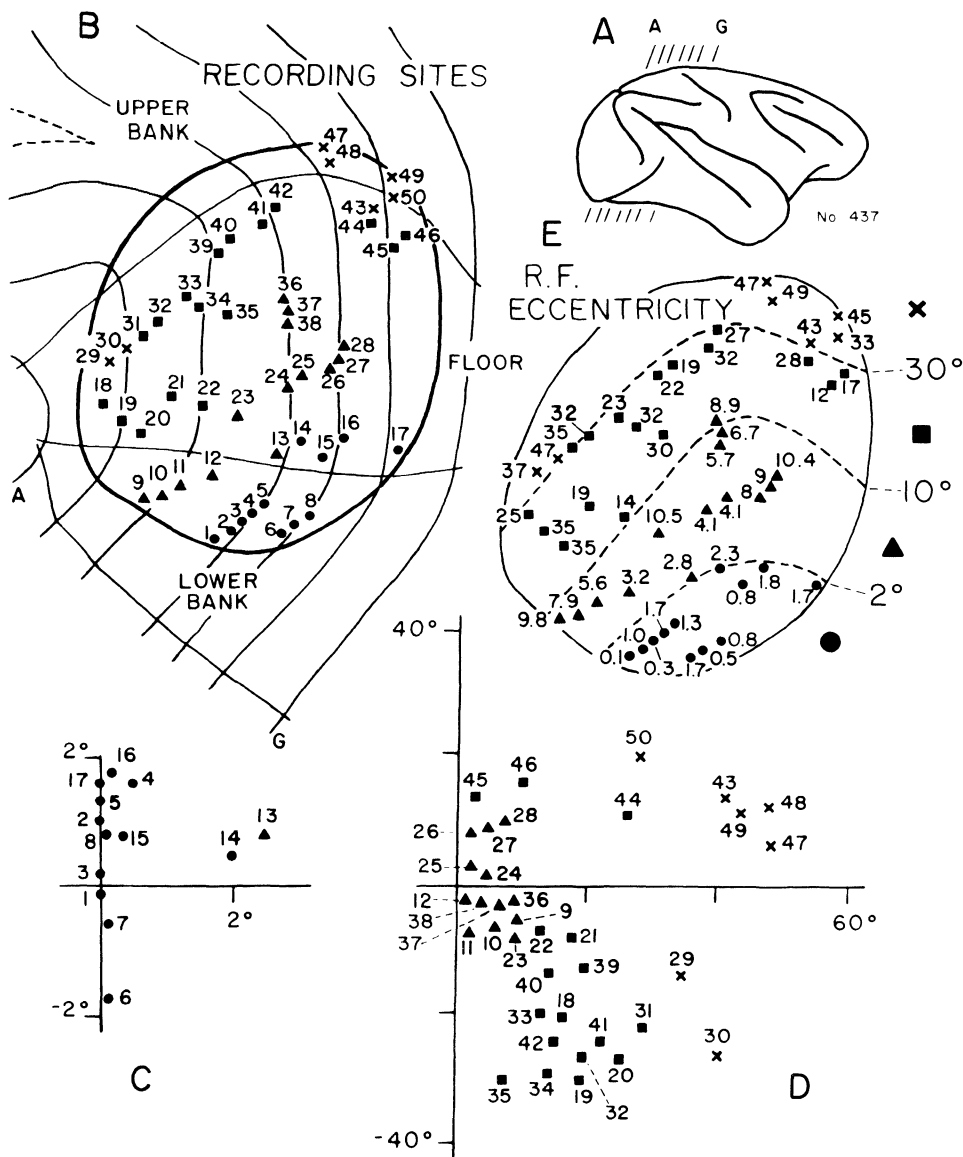


FIG. 4. Steps in the production of a map of the visual topography of MT for animal 437. *A*: lateral view of hemisphere showing level of sections used to construct a three-dimensional model of a portion of STS. *B*: flattened model showing the limits of MT (thick line) determined on myeloarchitectonic criteria and the recording sites (numbered symbols). Lines A-G were traced from the flattened sections and the thin lines crossing them indicate (from top to bottom) the junction between the floor and upper bank, the junction between the floor and lower bank, and the lip of the lower bank. *C* and *D*: location of centers of the receptive fields recorded at the sites indicated in *A*. Central sites are shown in *C* and more peripheral ones in *D*. Numbers refer to the recording sites shown in *A*. *E*: numbers indicate the eccentricity in degrees of the receptive-field centers at the sites indicated by symbols. The dashed lines are isoeccentricity lines drawn on the basis of values shown for the individual sites. In all parts of the figure, dots, triangles, squares, and crosses refer to the location of the recording sites with respect to the isoeccentricity lines drawn in *E*.

greatly magnified relative to the representation of the periphery. Furthermore, the portion of MT devoted to the lower visual

field is greater than that devoted to the upper visual field.

Examination of Fig. 4 reveals consider-

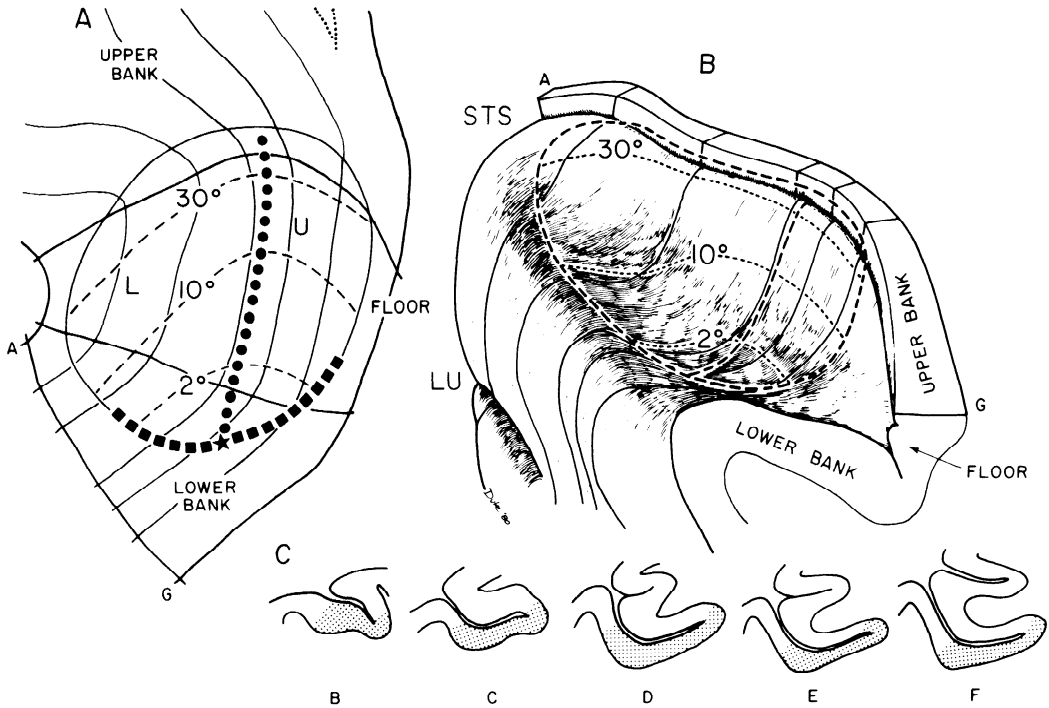


FIG. 5. MT in animal 437. *A*: flattened model showing the representation of the vertical meridian (squares), of the horizontal meridian (circles), and of the center of gaze (star) and isoeccentricity lines (dashed lines). L and U, representation of the lower and upper visual fields, respectively. *B*: three-dimensional drawing showing borders and meridians (large dashes) and isoeccentricity lines (small dashes). *C*: sections *B*–*F* showing the location of MT (gray).

able local “disorganization,” “scatter,” or “coarseness” in the topographical organization of receptive-field centers. That is, the location of receptive-field centers at several sites deviates from the overall organization represented by the meridians and isoeccentricity lines drawn on the maps. (For example, sites 6, 19, 20, 37, 45, and 46 in Fig. 4.) In order to represent the amount of scatter, the location of the isoeccentricity lines intermediate to the vertical meridian and the 2, 10, and 30° isoeccentricity lines were estimated on the basis of the cortical magnification factor (see below). The experimentally derived eccentricities for each recording site were then plotted against the ones expected from the full set of isoeccentricity lines. To the extent that these isoeccentricity lines are an accurate summary of the eccentricity values actually obtained, the best-fitting straight line through such a plot should be a 45° line through the origin. Further-

more, the distribution of individual points about the line provides a measure of scatter or coarseness of the representation. If there were no scatter, all the points should fall on the line. Such a plot is shown in Fig. 8. The line fitted with the method of least squares had a slope of 1.03 and intersected the *y* axis near the origin, indicating the adequacy of the isoeccentricity lines fitted by eye. Furthermore, note that the scatter (i.e., deviation of individual points from the regression line) was much greater beyond an eccentricity of 15°. Since receptive-field size also increases with eccentricity, we examined the relationship between scatter and receptive-field size. As shown in Fig. 9, the ratio of scatter (i.e., deviation from the regression line in Fig. 8) to square root of receptive-field area does not vary with eccentricity. Thus, increasing receptive-field size appears to be the major basis of increasing scatter with increasing eccentricity. By contrast, the

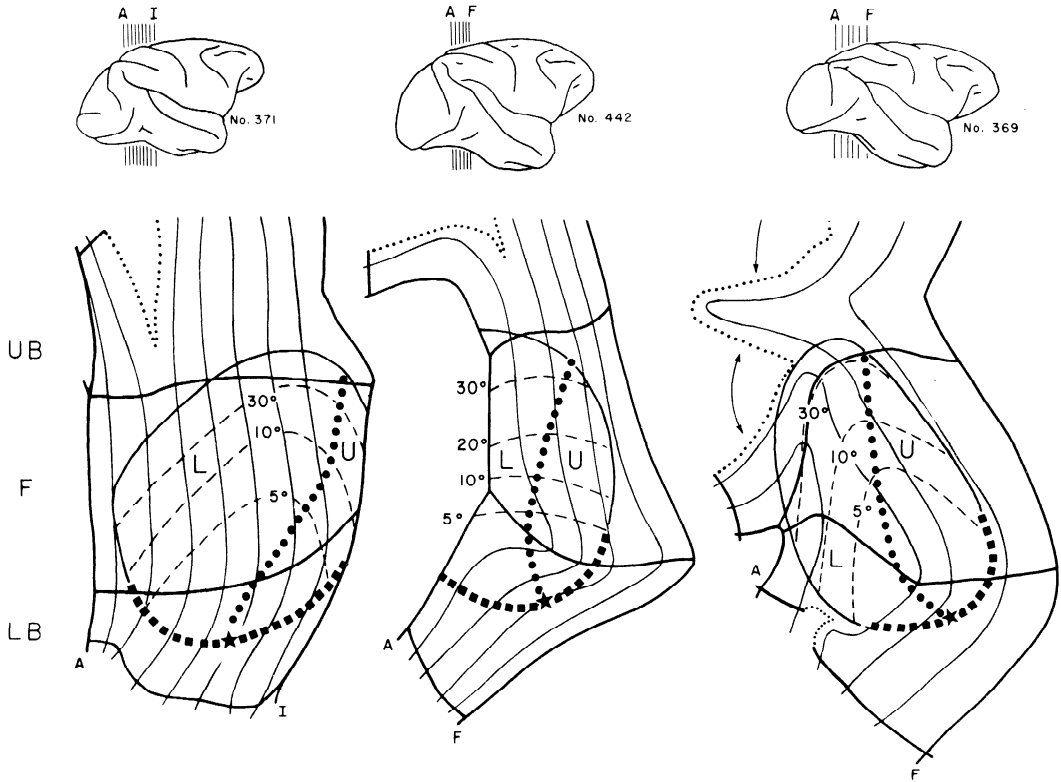


FIG. 6. Visual topography of MT in three additional animals. Lateral views of hemispheres indicating levels of sections are shown above and the flattened models made from each set of sections below. The dotted lines indicate where the cross pieces of the three-dimensional model had to be cut in order to flatten it. On each flattened model the vertical meridian (squares), the horizontal meridian (circles), the center of gaze (stars), the isoeccentricity lines (dashed), and the upper (U) and lower (L) visual fields are shown.

amount of scatter did not appear to be related to the cortical layer of the recording site or to response properties such as directionality (to the extent they could be assessed with multiunit recording). Furthermore, at a given eccentricity, there was no relation between receptive-field size and scatter.

Receptive-field area and eccentricity

Receptive-field size (square root of receptive-field area) is plotted as a function of eccentricity of receptive-field center for animal 437 in Fig. 10. As noted earlier, receptive-field size grows markedly with increasing eccentricity. In order to compare this function with those previously obtained for other visual areas under the same multiunit-recording conditions, a straight line was fitted to the data with the method of least

squares. The slope for MT (0.91) was significantly greater than that obtained under similar conditions for V1 (0.16) and V2 (0.40) ($t = 14.6$, $P < 0.001$; $t = 9.5$, $P < 0.001$, respectively) (12). The y intercept of the regression line was also higher for MT than for either V1 or V2. Thus, receptive-field size at a given eccentricity is larger in MT than in both V1 and V2 and it increases more rapidly with increasing eccentricity.

In MT (and also in V1 and V2), receptive fields obtained under our multiunit-recording conditions are larger than those obtained with single-unit recording. Thus, the function relating receptive-field size and eccentricity for isolated single neurons in MT has a similar y intercept but a smaller slope than that obtained with multiunit electrodes under identical conditions in a similar portion

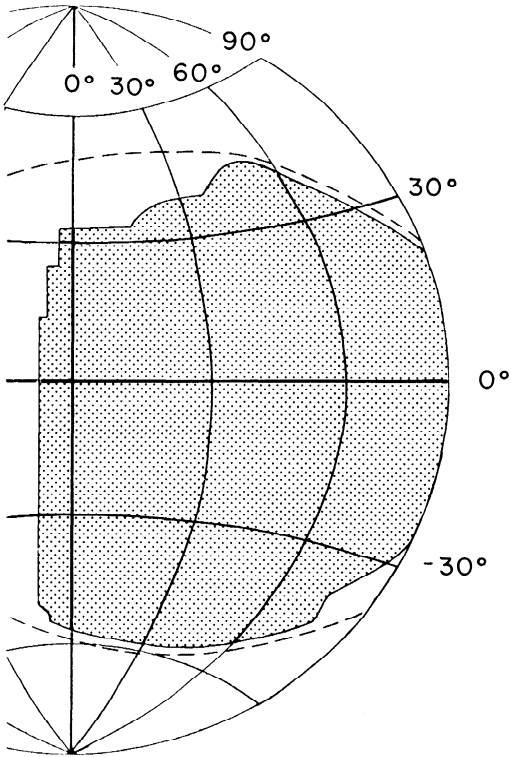


FIG. 7. Extent of visual field represented in MT of animal 437 (gray). The dashed line indicates the extent of the visible visual field.

of MT (T. Albright and R. Desimone, unpublished data). Similarly, the slope of this function for V1 obtained with single-neuron electrodes (16) is slightly smaller than that obtained with multiunit recording (12).

Cortical magnification and eccentricity

Cortical magnification, i.e., the distance in millimeters between two recording sites divided by the distance in degrees between the centers of the receptive fields recorded at those sites (7) is plotted as a function of eccentricity in Fig. 11. Note that cortical magnification is very high near the fovea and decreases very slowly beyond 10° .

In order to compare cortical magnification in MT with that of other visual areas, the best-fitting power function was obtained with the method of least squares. Its equation was $M = 4.3E^{-1.4}$ where M is the cortical magnification and E , retinal eccentric-

ity. In the inset of Fig. 11, this power function is compared on a log scale with that previously obtained under similar conditions in V1 (12). The slopes of the two functions were not significantly different ($t = 1.35$, $P > 0.05$) suggesting convergence from sites of V1 into MT, resulting in a logarithmic compression. The lower intercepts for MT parallel its much smaller area. The area of MT as determined on the myeloarchitectonic criteria described in the next section were 72.9 mm^2 (animal 369), 80.6 mm^2 (442), 82.6 mm^2 (371), 96.3 mm^2 (437), (mean, 83.1 mm^2). (We were unable to determine reliably the dorsal border of MT in the other two animals.) By contrast, our estimates for the area of V1 in two animals were 900 and 746 mm^2 (12). Thus, the visual topography of MT is a marked compression of that of V1 but maintains the same organization.

Architectonic correlates of MT

The borders of MT on physiological criteria (reversal in receptive-field progression and sometimes a sharp change in receptive-field size) could be determined to no closer than 0.4–1.5 mm, since recording sites on

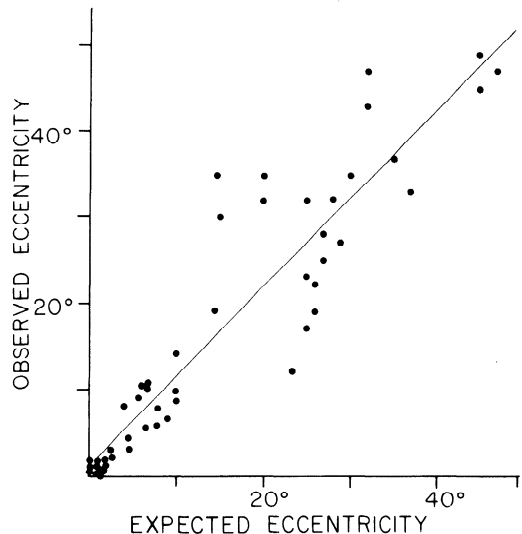


FIG. 8. Scatter of receptive-field centers in animal 437. The observed eccentricities of the receptive-field centers are plotted against eccentricities expected on the basis of the map shown in Fig. 5A and the best-fitting line drawn through points.

a single penetration were at least 0.4 mm apart and between adjacent penetrations at least 1–1.5 mm apart. Within these limits, the border of MT electrophysiologically determined corresponded to a myeloarchitectonic transition.

The clearest myeloarchitectonic border was at the representation of the vertical meridian near the bottom of the lower bank of STS. In this region there is a heavy pattern of myelination from the bottom of layer III to layer VI that almost totally obscures the two prominent bands (of Baillarger) that characterize the cortex lateral to MT. The extent of this region of heavy myelination across the floor of STS is variable from animal to animal. However, it always appears to end between the 10 and 30° isoeccentricity lines determined electrophysiologically. The more peripheral portions of MT are less heavily myelinated than this central portion and the bands of Baillarger become more prominent. The arrows marked *b* in Figs. 2 and 3 indicate the transition between the heavily and more lightly myelinated areas within MT.

The border of the dorsal portion of MT, containing the representation of the periphery, is less clear than the ventral border. Dorsal and anterior, the myelination is much lighter than in the adjacent MT (Fig. 14). This area, with large receptive fields and no apparent topographic organization, is within Brodman's area 7. Dorsal and posterior, the density of myelination is similar to the ad-

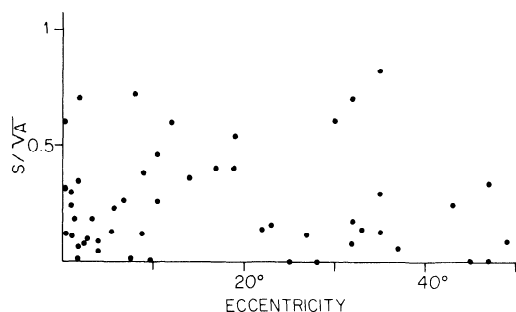


FIG. 9. Ratio of scatter to receptive-field size as a function of eccentricity for animal 437. Scatter is the absolute deviation of the observed eccentricity of the receptive-field center from the regression line shown in Fig. 8. Note that this ratio does not change as a function of eccentricity.

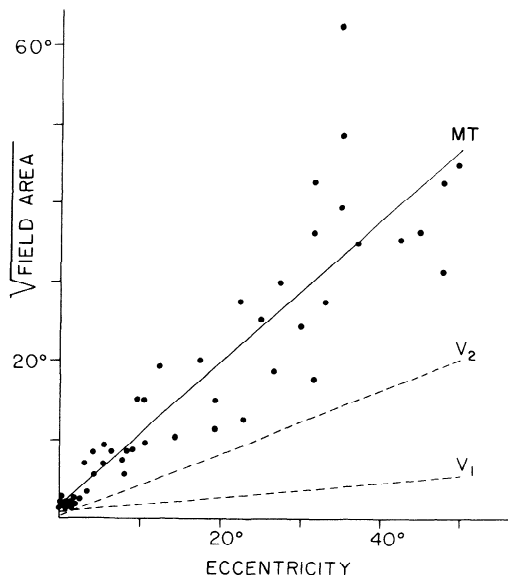


FIG. 10. Receptive-field size as a function of eccentricity of receptive-field center in animal 437. The dashed lines show the same function for V1 and V2.

adjacent MT but the inner band of Baillarger is thicker (Fig. 14). (This area corresponds to Zeki's (38) V4.) In some sections from some animals this border could only be determined to within 2 mm.

The correlation between visual topography and myeloarchitecture in a coronal section is illustrated in Figs. 12 and 13. Note the transition to a pattern of heavy myelination at *a* at the lateral border of MT. At *b*, at the medial border, the myelination becomes lighter again.

Figure 14 illustrates the fiber pattern in a sagittal section. The ventral portion containing the representation of the central 10° shows a pattern of heavy myelination obscuring the bands of Baillarger. At *a* in the anterior bank there is a transition to a more lightly myelinated area corresponding to the border of MT with area 7. At *b* in the posterior bank, the myelination becomes light at a point corresponding to an eccentricity of about 15°. This pattern of myelination continues to *c* at the border of MT with V4. Within V4, the inner band of Baillarger is thicker than in MT. (The visual topography of an adjacent section from this animal is shown in Fig. 3.)

We were unable to distinguish MT using

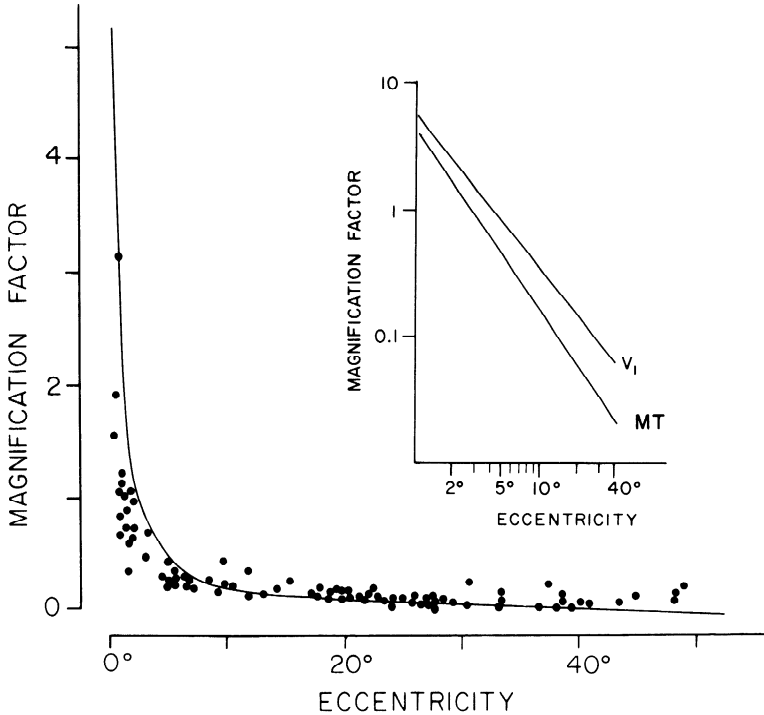


FIG. 11. Magnification factor in millimeters per degree as a function of eccentricity for animal 437. The insert shows, on a log scale, this function for MT and that previously obtained for V1.

cytoarchitectonic criteria. As Ungerleider and Mishkin (32) have pointed out, it falls within Brodman's area 19 and the ventral portion is within von Bonin and Bailey's (34) area OA and the dorsal portion within area PG.

DISCUSSION

Visual topography

We have described the visuotopic organization of the striate-recipient zone in the posterior portion of the superior temporal sulcus of the macaque (MT). It contains a complete representation of the contralateral visual field. The representation of the central portion of the vertical meridian forms the lateral border and lies in the lower bank of STS and that of the horizontal meridian crosses the floor of STS, with the representation of the upper visual field anteroventral and that of the lower visual field postero-dorsal. Thus, in Allman and Kaas' (2) terminology, MT like V1, is a first-order transformation of the visual field. It differs from

V1 in its much smaller size, in its relatively larger representation of the lower visual field than the upper visual field, in its cruder topography, and in its much larger receptive fields.

There are several consequences (or concomitants) of the large receptive fields in MT. The first is that some fields extend up to 10° into the ipsilateral half-field. Second, beyond an eccentricity of about 5°, there are no receptive-field centers on or near the vertical meridian. Rather, most of the vertical meridian is represented by neurons that have receptive fields with centers 5–20° from the vertical meridian but whose medial borders extend to or across the vertical meridian. Third, although there are virtually no receptive-field centers beyond an eccentricity of 50°, the extreme periphery of the visual field is represented by very large receptive fields whose centers may have an eccentricity of only 30–40°. Finally, we suggest that the scatter or crudeness of the visual topography of MT is related to its large receptive fields. That is, the situation in MT appears fun-

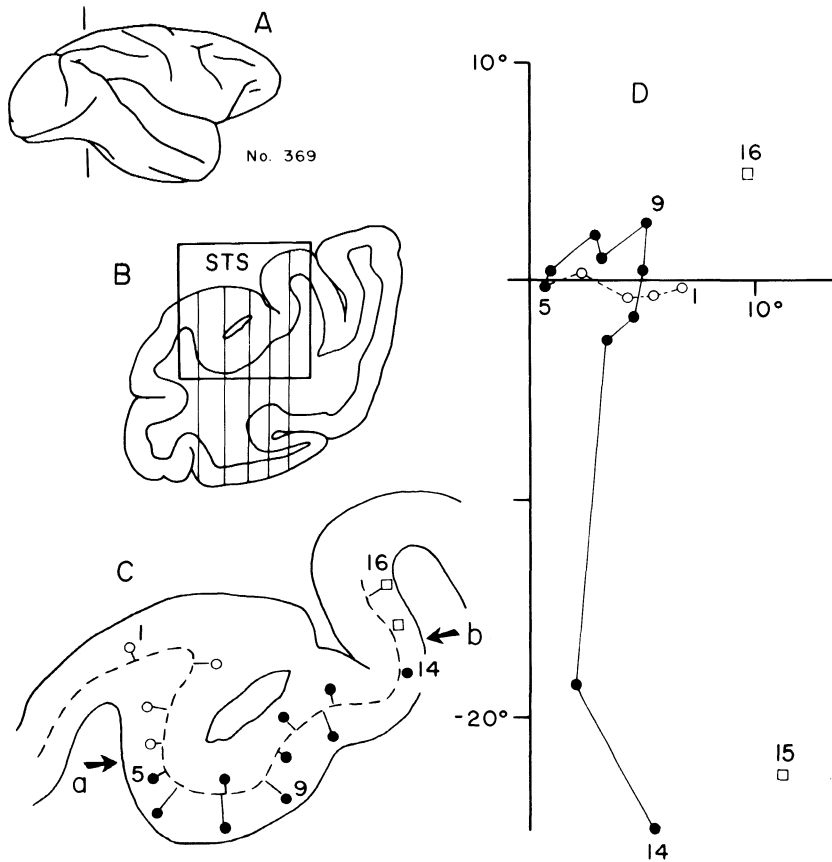


FIG. 12. Receptive-field centers in MT and adjacent areas in a series of penetrations in the coronal plane. *A*: lateral view of the brain showing level of the section. *B*: coronal section showing electrode tracks and the portion enlarged in *C*. *C*: enlarged portion of STS indicating the recording sites outside (open squares and circles) and inside (filled circles) MT projected onto layer IV (dashed line). Limits of MT determined by myeloarchitectonic criteria are shown by arrows *a* and *b*. *D*: receptive-field centers recorded at the sites shown in *C*. A photomicrograph of this section stained for fibers is shown in Fig. 13.

damentally the same as in V1, where scatter and field size parallel each other (16). In fact, although the scatter of receptive fields at a given eccentricity is much greater in MT than in V1, if we equate for receptive-field size, scatter in V1 and MT is actually quite similar.

Two groups of investigators have commented previously on the organization of MT on the basis of single-neuron recording. Dubner and Zeki (10) noted that the topographic organization "is crude and essentially quadratic", and later Zeki (40) wrote that it is "relatively crude compared . . . to area 17," and still later (43) that "some parts of the field are multiply represented." Each of these studies appears to involve only

a few penetrations through MT in individual animals. As may be seen from Fig. 4, this amount of sampling within MT is simply insufficient to reveal its topographic properties. On many of our single penetrations, the progression of receptive fields was certainly not smooth (as compared to V1 and V2) and occasionally contained reversals ("multiple representations") and "anomalous" fields, particularly at eccentricities beyond 10°. At least a dozen penetrations in a single animal were required to establish the topography in even parts of MT and even more for a relatively complete map. It is also possible that multiunit recording may reveal topography more easily than single-unit recording.

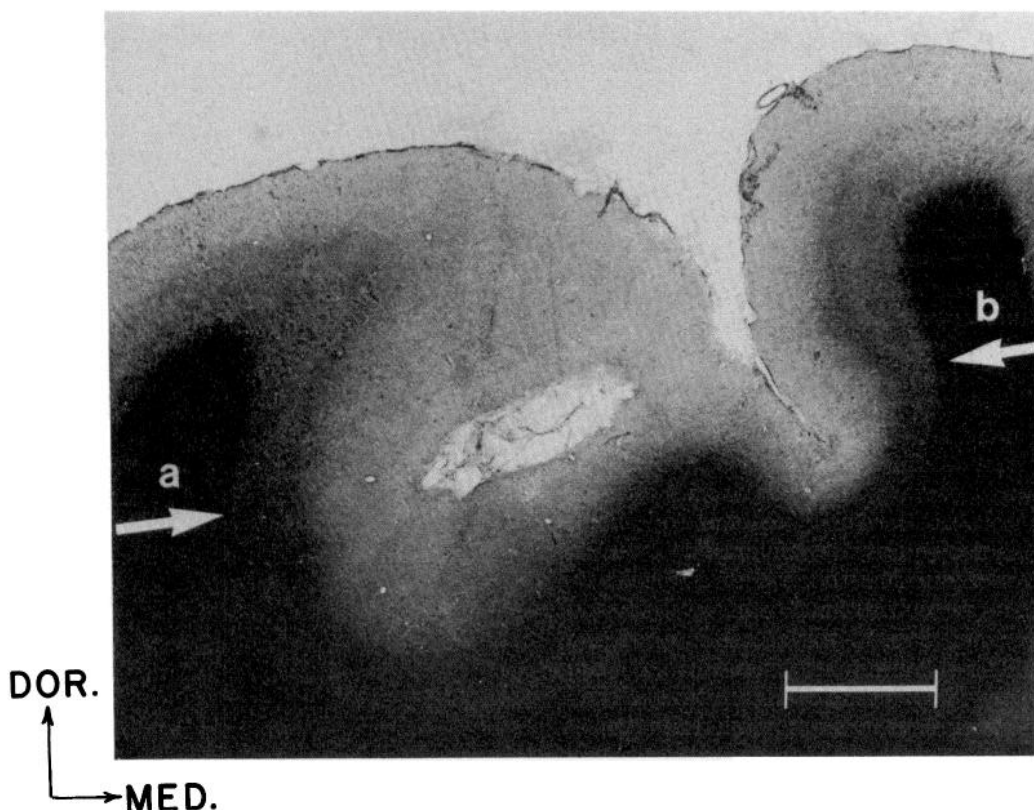


FIG. 13. Photomicrograph of the portion of the coronal section shown in Fig. 12C stained for fibers. Arrows a and b indicate borders of MT and the bar, 2 mm.

Maunsell, Bixby, and Van Essen (22) noted that receptive fields of cells on the edge of MT are not always close to the perimeter of the visual field and that relatively large shifts in receptive-field locations sometimes occur over short distances. Both observations are similar to our own (e.g., Fig. 4).

There are several interesting questions that our methods were unable to answer. Our electrode penetrations were very rarely orthogonal to the cortical surface, nor did we record at sites less than 400 μm apart. Thus, we were unable to test for laminar differences in topography or receptive-field size. Since we usually recorded from clusters of neurons, we could not study systematically the response properties of MT units. However, it was very clear that the multiunit clusters were sensitive to the direction of stimulus movement. The ability to observe this direction sensitivity with multiunit re-

coding probably reflects the fact that adjacent single neurons in MT tend to have similar directional selectivities (40, T. Albright and R. Desimone, unpublished observations). By contrast, the multiunit clusters usually appeared insensitive to the form, color, and size of the stimulus. In general, the response properties we observed with multiunit recording were similar to those previously reported by Dubner and Zeki (10) and Zeki (40, 42, 43) for single neurons.

MT is surrounded by visually responsive cortex. Dorsal and posterior, corresponding to Zeki's V4, the receptive fields are topographically organized. The cortex ventral to MT also appears to be retinotopically organized, but its relation to V4 is unclear. Finally, dorsal and anterior within Brodman's area 7, the receptive fields are very large and do not appear to be retinotopically organized.

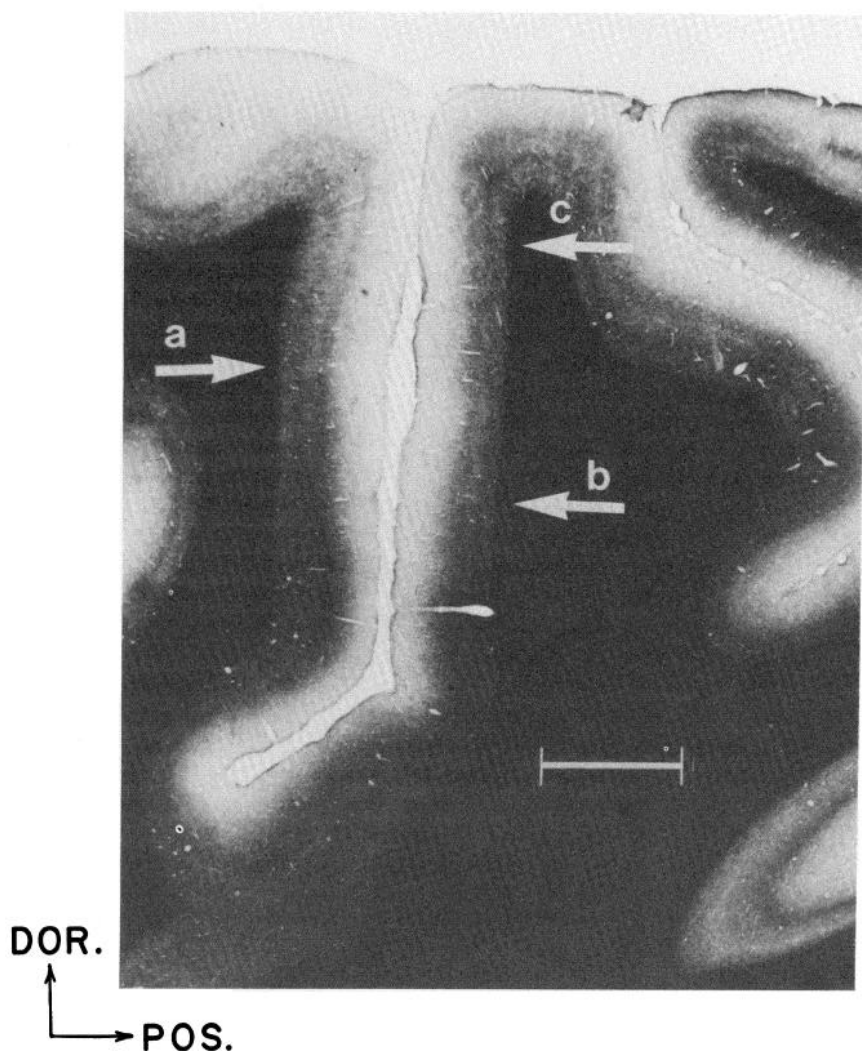


FIG. 14. Photomicrograph of a portion of a sagittal section through STS stained for fibers. Arrows a and c show limits of MT and arrow b indicates the transition from heavy (below) to lighter myelination within MT. The bar indicates 2 mm. This section was 2 mm medial to the one drawn in Fig. 3.

Relation to anatomical studies

Ungerleider and Mishkin (32) studied the topography of the striate projections to STS by making partial lesions of striate cortex and processing the brains for anterograde degeneration. Collectively, the lesions included all of striate cortex. The total area of degeneration in STS corresponded in location and area to the area we defined as MT on electrophysiological and myeloarchitectonic grounds. The partial lesions of

striate cortex included cortex representing the center, the periphery, or the far periphery of the visual field. They found that the portion of striate cortex representing the central 7° projects to the ventral border of MT at the bottom of the lower bank of STS, that the more peripheral representation in the calcarine sulcus projects to the junction of the floor and upper bank of STS. That is, within the limits of their methods, the topography of the striate projections to MT

corresponded exactly with the representation of the visual field revealed by our multiunit mapping (although they used *M. mulatta* and we used *M. fascicularis*). Rockland and Pandya (24), Weller and Kaas (35), and Montero (23) report having confirmed Ungerleider and Mishkin's (32) results, at least in general, with labeled amino acid anterograde tracing methods. Montero (23) and Rockland and Pandya (24) also noted that the projections from the representation of the upper visual field in striate cortex terminated in STS ventral and medial to those from the representation of the lower field.

Van Essen and his colleagues (22, 33) also studied striate projections to MT with anterograde transport methods and confirmed that the portions of striate cortex representing the center of the visual field project more ventrolaterally and those representing the periphery project more dorsomedially. They determined the area and location of MT on myeloarchitectonic criteria and arrived at a much smaller estimate (35 mm²) than either Ungerleider and Mishkin (32) or we (80 mm²) did. The reason for this discrepancy may be that their primary criterion for this area was a zone of heavy myelination in STS. We found that this heavily myelinated zone does not extend to the dorsal border of MT, as determined by the reversal of the progression of receptive-field centers. Furthermore, the dorsal, less heavily myelinated zone contains receptive fields that include peripheral portions of the visual field that are not included in the more ventral, heavily myelinated one. Similarly, Ungerleider and Mishkin found that this heavily myelinated zone does not extend to the dorsal border, as determined by the projections from striate cortex.

In each of the anterograde transport studies cited above, it was clear that the projection from striate cortex to MT is not a simple compressing of the striate map onto a region of STS. Single injections in striate cortex often result in multiple bands or patches of labeling in MT (22, 23, 36, 37). Furthermore, projections from separate sites in striate cortex may converge onto single sites in MT (23). It is tempting to suggest that these phenomena of single striate sites projecting to multiple sites in MT and multiple

striate sites projecting to single sites in MT may be related to the large receptive fields and local scatter in MT. Even if this is the case, it should be noted that single injections producing multiple sites of labeling do not seem to be unique to MT in the macaque but have been reported for striate-MT projections in other species, e.g., squirrel monkey (37) and owl monkey (23), and for connections among other visual areas, e.g., from V1 to V2 (36). These phenomena of divergence and convergence are presumably related to patterns of functional architecture that are superimposed on the basic visuotopic organization. For example, in MT, there appears to be a columnar organization for direction of movement (T. Albright and R. Desimone, unpublished data).

For at least some visual areas, the pattern of degeneration after cutting the corpus callosum reflects the representation of the vertical meridian. The callosal inputs to MT have been reported to be patchy, irregular, and not specifically concentrated along its perimeter (33). This is consistent with our finding that there are sites throughout MT that have receptive fields with medial borders that extend to or near the vertical meridian.

Relation to MT in other species

Several investigators have suggested that the striate-recipient zone in the posterior portion of the superior temporal sulcus of the macaque is homologous to the area designated as MT in other species of primates (1, 32, 33, 36). Among the arguments for this view are the following: 1) both areas are located in the rostral portion of Brodman's area 19 (2, 3, 27, 29), 2) in both areas the deeper layers of the portion containing the central representation are heavily myelinated (2, 32), 3) both areas have reciprocal topographically organized connections with striate cortex that arise from layer IVb and the giant cells of Meynert and terminate predominantly in the lower part of layer III and in layer IV (20, 21, 24–26, 29, 31, 32, 36), 4) single sites in striate cortex often project to separate loci in both areas (23, 33, 36, 37), 5) both areas receive a projection from V2 (18, 24, 30, 41), 6) neurons in layer

V of both areas project to the pontine visual nuclei (13, 14, 28), 7) both areas project to rostral cortex that is visually responsive but do not project directly to inferior temporal cortex (8, 27, 36), 8) neurons in both areas are particularly sensitive to the direction of movement and not to form or color (4, 40, 42).

The present finding that MT in the macaque, as in other species, is a first-order transformation further supports the homology of these areas. There are, of course, also differences between macaque MT and other MTs (cf. Ref. 44). The principal ones revealed by the present study are the larger receptive fields and the greater local scatter in topography in the macaque.

NOTE ADDED IN PROOF

A full account of Van Essen et al.'s study of MT referred to above (22, 33) has just appeared: VAN ESSEN, D. C., MAUNSELL, J. H. R., AND BIXBY, J. L. The

middle temporal visual area in the macaque: myeloarchitecture, connections, functional properties, and topographical organization. *J. Comp. Neurol.* 199: 293-326, 1981.

ACKNOWLEDGMENTS

We thank D. Dawson for preparing the figures and helping with the data analysis; S. Gorlick for assistance with histology; T. Albright, E. Covey, R. Desimone, M. Mishkin, A. P. B. Sousa, and L. Ungerleider for their comments on the manuscript; J. Kaas for information on the Heidenhain-Woelke stain; and K. Walsh for typing.

This study was supported by National Institutes of Health Grants MH-19420 and FOSTWO2855, National Science Foundation Grant BNS 79-05589, and Conselho Nacional de Desenvolvimento Científico e Tecnológico-Brazil Grant CNPq 1112. 1003/77.

Present address of R. Gattass: Dept. Neurobiologia Instituto de Biofísica, Centro de Ciências da Saúde, UFRJ, Ilha do Fundão, 21910 Rio de Janeiro RJ, Brazil.

Received 26 January 1981; accepted in final form 21 April 1981.

REFERENCES

1. ALLMAN, J. M. Reconstructing the evolution of the brain in primates through the use of comparative neurophysiological and neuroanatomical data. In: *Primate Brain Evolution: Methods and Concepts*, edited by E. Armstrong. New York: Plenum. In press.
2. ALLMAN, J. M. AND KAAS, J. H. A representation of the visual field in the caudal third of the middle temporal gyrus of the owl monkey (*Aotus trivirgatus*). *Brain Res.* 31: 85-105, 1971.
3. ALLMAN, J. M., KAAS, J. H., AND LANE, R. H. The middle temporal visual area (MT) in the bush-baby, *Galago senegalensis*. *Brain Res.* 57: 197-202, 1973.
4. BAKER, J. F., PETERSEN, S. E., NEWSOME, W. T., AND ALLMAN, J. M. Visual response properties of neurons in four extrastriate visual areas of the owl monkey (*Aotus trivirgatus*): a quantitative comparison of medial, dorsomedial, dorsolateral, and middle temporal areas. *J. Neurophysiol.* 45: 397-416, 1981.
5. BRUCE, C., DESIMONE, R., AND GROSS, C. G. Visual properties of neurons in a polysensory area in superior temporal sulcus of the macaque. *J. Neurophysiol.* 46: 369-384, 1981.
6. CRAGG, B. G. AND AINSWORTH, A. The topography of the afferent projections in the circumstriate visual cortex of the monkey studied by the Nauta method. *Vision Res.* 9: 733-747, 1969.
7. DANIEL, P. M. AND WHITTERIDGE, D. The representation of the visual field on the cerebral cortex in monkeys. *J. Physiol. London* 159: 203-221, 1961.
8. DESIMONE, R., FLEMING, J., AND GROSS, C. G. middle temporal visual area in the macaque: myeloarchitecture, connections, functional properties, and topographical organization. *J. Comp. Neurol.* 199: 293-326, 1981.
9. DESIMONE, R. AND GROSS, C. G. Visual areas in the temporal cortex of the macaque. *Brain Res.* 178: 363-380, 1979.
10. DUBNER, R. AND ZEKI, S. M. Response properties and receptive fields of cells in an anatomically defined region of the superior temporal sulcus in the monkey. *Brain Res.* 35: 528-532, 1971.
11. GATTASS, R. AND GROSS, C. G. A visuotopically organized area in the posterior superior temporal sulcus of the macaque (Abstract). *Invest. Ophthalmol. Suppl.* 18: 184, 1979.
12. GATTASS, R., GROSS, C. G., AND SANDELL, J. H. Visual topography of V2 in the macaque. *J. Comp. Neurol.* In press.
13. GLICKSTEIN, M., COHEN, J., ROBINSON, F., AND GIBSON, A. Cortical visual inputs to the monkey pons (Abstract). *Invest. Ophthalmol. Suppl.* 17: 292, 1978.
14. GRAHAM, J., LIN, C.-S., AND KAAS, J. H. Subcortical projections of six visual cortical areas in the owl monkey, *Aotus trivirgatus*. *J. Comp. Neurol.* 187: 557-580, 1979.
15. GROSS, C. G., BRUCE, C. J., DESIMONE, R., FLEMING, J., AND GATTASS, R. Three visual areas of the temporal lobe. In: *Multiple Cortical Areas*, edited by C. N. Woolsey. Englewood Cliffs, NJ: Humana. In press.
16. HUBEL, D. H. AND WIESEL, T. N. Uniformity of monkey striate cortex: a parallel relationship between field size, scatter and magnification factor. *J. Comp. Neurol.* 158: 295-306, 1974.
17. JONES, E. G. AND POWELL, T. P. S. An anatomical

- study of converging sensory pathways within the cerebral cortex of the monkey. *Brain* 93: 793-820, 1970.
18. KAAS, J. H. AND LIN, C.-S. Cortical projections of area 18 in owl monkeys. *Vision Res.* 17: 739-741 1977.
 19. KUYPERS, H. G., SZWARCART, M. K., MISHKIN, M., AND ROSVOLD, H. E. Occipito-temporal cortico-cortical connections in the rhesus monkey. *Exp. Neurol.* 11: 245-262, 1965.
 20. LUND, J. S., LUND, R. D., ENDRICKSON, A. E., BUNT, A. H., AND FUCHISI, A. F. The origin of efferent pathways from the primary visual cortex, area 17, of the macaque monkey as shown by retrograde transport of horseradish peroxidase. *J. Comp. Neurol.* 164: 287-305, 1975.
 21. MARTINEZ-MILLAN, L. AND HOLLANDER, H. Cortico-cortical projections from striate cortex of the squirrel monkey (*Saimuri sciureus*). A radio-autographic study. *Brain Res.* 83: 405-417, 1975.
 22. MAUNSELL, J. H. R., BIXBY, J. L., AND VAN ESSEN, D. C. The middle temporal area (MT) in the macaque: architecture, functional properties and topographic organization. *Soc. Neurosci. Abstr.* 5: 796, 1979.
 23. MONTERO, V. M. Patterns of connections from the striate cortex to cortical visual areas in superior temporal sulcus of macaque and middle temporal gyrus of owl monkey. *J. Comp. Neurol.* 189: 45-55, 1980.
 24. ROCKLAND, K. S. AND PANDYA, D. N. Cortical connections of the occipital lobe in the rhesus monkey: interconnections between areas 17, 18, 19 and the superior temporal sulcus. *Brain Res.* 212: 249-270, 1981.
 25. SPATZ, W. B. Thalamic and other subcortical projections to area MT (visual area of superior temporal sulcus) in the marmoset *Callithrix jacchus*. *Brain Res.* 99: 129-134, 1975.
 26. SPATZ, W. B. Topographically organized reciprocal connections between areas 17 and MT (visual area of superior temporal sulcus) in the marmoset *Callithrix jacchus*. *Exp. Brain Res.* 27: 559-572, 1977.
 27. SPATZ, W. B. AND TIGGES, J. Experimental-anatomical studies on the "middle temporal visual area (MT)" in primates. I. Efferent cortico-cortical connections in the marmoset *Callithrix jacchus*. *J. Comp. Neurol.* 146: 451-464, 1972.
 28. SPATZ, W. B. AND TIGGES, J. Studies of the visual area MT in primates. II. Projection fibers to subcortical structures. *Brain Res.* 61: 374-378, 1973.
 29. SPATZ, W. B., TIGGES, J., AND TIGGES, M. Subcortical projections, cortical associations, and some intrinsic interlaminar connections of the striate cortex in the squirrel monkey (*Saimiri*). *J. Comp. Neurol.* 140: 155-174, 1970.
 30. TIGGES, J., SPATZ, W. B., AND TIGGES, M. Efferent cortico-cortical fiber connections of area 18 in the squirrel monkey (*Saimiri*). *J. Comp. Neurol.* 158: 219-236, 1974.
 31. TIGGES, J., TIGGES, M., AND KALAH, C. S. Efferent connections of area 17 in *Galago*. *Am. J. Phys. Anthropol.* 38: 393-397, 1973.
 32. UNGERLEIDER, L. AND MISHKIN, M. The striate projection zone in the superior temporal sulcus of *Macaca mulatta*: location and topographic organization. *J. Comp. Neurol.* 188: 347-366, 1979.
 33. VAN ESSEN, D. C., MAUNSELL, J. H. R., AND BIXBY, J. L. The organization of extrastriate visual areas in the macaque monkey. In: *Multiple Cortical Areas*, edited by C. N. Woolsey. Englewood Cliffs, NJ: Humana. In press.
 34. VON BONIN, G. AND BAILEY, P. *The Neocortex of Macaca mulatta*. Urbana: University of Illinois Press, 1947.
 35. WELLER, R. E. AND KAAS, J. H. Connections of striate cortex with the posterior bank of the superior temporal sulcus in macaque monkeys. *Soc. Neurosci. Abstr.* 4: 650, 1978.
 36. WELLER, R. E. AND KAAS, J. H. Cortical and subcortical connections of visual cortex in primates. In: *Multiple Cortical Areas*, edited by C. N. Woolsey. Englewood Cliffs, NJ: Humana. In press.
 37. WONG-RILEY, M. Columnar cortico-cortical interconnections within the visual system of the squirrel and macaque monkeys. *Brain Res.* 162: 201-217, 1979.
 38. ZEKI, S. M. Representation of central visual fields in prestriate cortex of monkey. *Brain Res.* 14: 271-291, 1969.
 39. ZEKI, S. M. Convergent input from the striate cortex (area 17) to the cortex of the superior temporal sulcus in the rhesus monkey. *Brain Res.* 28: 338-340, 1971.
 40. ZEKI, S. M. Functional organization of a visual area in the posterior bank of the superior temporal sulcus of the rhesus monkey. *J. Physiol. London* 236: 549-573, 1974.
 41. ZEKI, S. M. The projections to the superior temporal sulcus from areas 17 and 18 in the rhesus monkey. *Proc. R. Soc. London Ser. B* 193: 199-207, 1976.
 42. ZEKI, S. M. Uniformity and diversity of structure and function in rhesus monkey prestriate visual cortex. *J. Physiol. London* 277: 273-290, 1978.
 43. ZEKI, S. M. Functional specialization in the visual cortex of rhesus monkey. *Nature London* 274: 423-428, 1978.
 44. ZEKI, S. M. The response properties of cells in the middle temporal area (area MT) of owl monkey visual cortex. *Proc. R. Soc. London Ser. B* 207: 239-248, 1980.